Design and characterization of asymmetric supercapacitor useful in hybrid energy storage systems for electric vehicles

Farshad Barzegar*, Damilola Momodu, Lijun Zhang*, Xiaohua Xia*, Ncholu Manyala****

** Electrical, Electronic and Computer Engineering Department, University of Pretoria, Pretoria 0002, South Africa (e-mail: farshadbarzegar@gmail.com).*

*** Physics Department, Institute of Applied Materials, SARCHI Chair in Carbon Technology and Materials, University of Pretoria, Pretoria 0028, South Africa (e-mail: ncholu.manyala@up.ac.za).*

Abstract:

Energy storage systems (ESSs) of electric vehicles (EVs) require high energy density and high power density concurrently. The ESSs with only supercapacitors (SCs) or high performance batteries (hpBs) have egregious limitations, and are unable to meet up the demands for specific power and energy concurrently. This study reports on the design and characterization of asymmetric supercapacitor based on activated carbon (ACC) and MoS_2 that suitable for use in hybrid energy storage systems in electric vehicles. The contribution of the double storage mechanism processes obtained from the faradaic storage sulfide material (MoS_2) combined with the excellent electric double layer storage from the activated carbon led to the overall realization of an specific energy of ~ 27.82 Wh kg^{-1} with a related specific power of 1000 W kg^{-1} at a 0.5 A g^{-1} gravimetric current density. In addition, the device also exhibited a 100% coulombic efficiency even after cycling for 10,000 continuous charge-discharge cycles serving as the highest reported presently on this device type. This shows the unique potential of adopting such ACC/MoS_2 materials as exceptional candidates to act as SC cells in the hybrid system for energy storage in electric vehicles.

Keywords: energy storage, hybrid system, activated carbon, MoS_2, supercapacitor

1. INTRODUCTION

The increasing energy demand in various advanced technological applications today and the dwindling state of the environment as a result of energy exploration/generation have necessitated the need to develop a reliable and robust energy storage system. Although there has been a growing trend in the investment into research for renewable energy generation to meet this skyrocketing demand, most of these new renewable resources are plagued by limitations based on natural phenomena like environmental and geographical factors. Thus, in order to maximally capture energy generated from these renewable resources when available, there is a need to have efficient storage systems which could preserve such energy for use whenever and wherever it is required. This also aids in preventing wastage of the excess generated energy.

Electrochemical capacitors (ECs) also referred to as supercapacitors (SCs) have become a great candidate for high power applications in energy storage units which bridge the gap between conventional capacitors and batteries. This is because of their relatively higher specific energy compared to normal parallel plate capacitors, and higher power density and longer cycling stability in comparison to batteries. The additional merits attributed to ECs in terms of the minimal or no extra maintenance cost as well as no special charging or control systems for operation further makes them of great interest to researchers (Conway 1999). The main backbone that determines an efficient energy storage device lies in the nature of the electrode materials adopted in designing them.

Considerable progress has been made into developing high performance materials for use in SCs with enhanced energy storing capability and electrochemical performance. The materials used for fabricating electrodes of SCs based on their charge storing mechanism can be divided into two main groups namely; electric double layer capacitor (EDLC) materials and pseudocapacitor (PC or redox capacitor) materials. The former stores electrical energy through continuous adsorption/desorption of ions at the electrode/electrolyte interface while the latter works mainly on fast reversible oxidation-reduction reactions at the active material surface (Simon & Gogotsi 2008). EDLCs are mainly composed of carbon-based materials like activated carbon (Frackowiak 2007) whereas PCs are mainly composed of transitional metal oxide/hydroxides and conducting polymers (Patil et al. 2015). Various scholars in the energy storage field have from early stages of SC research resorted to strategically combining the two types of supercapacitive storage modes in a single composite material (Zheng 1999; Wang et al. 2014) or in a single device resulting in a hybrid/asymmetric supercapacitor device (Jose et al. 2016; Conway 1999). The idea behind combining both material types is to tap out the merits of both materials in an attempt at improving the whole electrochemical performance of the composite. While the EDLC materials have good porous structure with high specific surface area (SSA) for efficient

cyclic stability, they are however characterized by a lower specific capacitance as compared to PC materials which can deliver a high specific capacitance but are less stable with a lower energy density (Li et al. 2016). For example, Y. Sato and co-workers (Sato et al. 2000) decorated activated carbon with small amounts of RuO_2 to increase its capacitance significantly. Owing to the cost and toxicity of the RuO_2, small amounts were used to obtain a carbon based composite material with the improved electrochemical property. Other approaches have also been explored to achieve higher specific capacitance, energy density, and overall device cycling stability. A method commonly adopted today is to combine transition metal oxides/hydroxides and transitional metal sulfides with carbonaceous materials. Most of these metal oxides and sulfides are characterized by a porous layered structure which aids ionic diffusion when the electrode material is in contact with the electrolyte (F. Barzegar et al. 2015; Bello et al. 2015; Zhang et al. 2008; Chen et al. 2010). Presently, metal sulfides such as CoS_2 (Ray et al. 2015), Ni_3S_2 (Li et al. 2015), and MoS_2 (Soon & Loh 2007) in particular, which exhibit a unique layered structure, are promising materials anticipated to have excellent capacitive properties due to the flake-like structure providing the necessary surface area for charge storage process to occur. Charge storage in MoS_2 thin films have been reported to occur in three main modes (Soon & Loh 2007): (i) inter-sheet double layer charge storage (ii) intra-sheet double layer storage on each MoS_2 layer through basal edge diffusion and (iii) redox transfer of charges via the Mo transition metal centre which exhibits variable oxidation state from +2 to +6 similar to RuO_2.

Unfortunately, even with such promising properties attributed to the MoS_2 material, there is still the problem of stability of this electrode material when adopted for supercapacitor applications. Although some studies have illustrated the enhancement of the whole capacitance of MoS_2 nanowalls due to the existence of a double layer capacitance along with faradaic capacitance during the diffusion of ions into the films at low scan rates, there are still few reports which have actually studied the merits of combining this material in an asymmetric device configuration with activated carbon electrodes.

Energy storage systems (ESSs) play a significant role in the economic benefits and power performance of electric vehicles (EVs). The ESSs with only SCs or batteries have notable limitations, and cannot meet the demands of energy density and power density of EVs concurrently. Mostly, batteries have high energy density but low power density. The SCs, on the other hand, have high power density but low energy density. Therefore, a hybrid energy storage system (HESS) combining batteries and SCs is one of the promising solutions for the ESSs used in applications that require both high energy density and power density, such as EVs.

This study reports the synthesis, design, and characterization of materials for an asymmetric supercapacitor that can be used in a hybrid energy storage system for electric vehicles. The contribution of the double storage mechanism process obtained from the sulphide material (MoS_2) combined with the excellent electric double layer storage process from the activated carbon led to the overall realisation of an energy density of over 27.82 Wh kg^{-1} with a specific power value of 1000 W kg^{-1} at a 0.5 A g^{-1}gravimetric current density. In addition, the device also exhibited a 100% coulombic efficiency even after cycling for 10,000 continuous charge-discharge cycles. Up to date, this serves as the highest reported so far for this type of devices. This shows the unique potential of adopting such ACC/MoS_2 materials as exceptional candidates in a SC cell adoptable in hybrid energy storage system for EVs.

2. Experimental

Coconut shell based activated carbon (ACC) was prepared by the following procedure. 10 g of KOH was mixed with 10 g of washed coconut shell and carbonized at 700 °C at 5 °C/minute, in argon gas atmosphere for 2 h. The carbonized sample was washed using 1 M HCl to eradicate the remaining KOH, followed by rinsing with deionized water (DI) to attain a neutral PH and the sample was dried at 60 °C. MoS_2 was prepared by a hydrothermal method (F. Barzegar et al. 2015). Firstly, ammonium paramolybdate ($(NH_4)_6Mo_7O_{24}\cdot 4H_2O$) and sodium diethyldithiocarbamate ($(C_2H_5)_2NCS_2Na\cdot 3H_2O$) were dissolved with stirring for a period of 12 h in deionized water. The solution was kept immobile under ambient condition for an additional 12 h period. After filtration, the solution containg a yellow precipitate ($Mo((C_2H_5)_2NCS_2)_2O_2$) was collected and rinsed with DI. Therafter, the collected powder was mixed with deionized water and placed into a stainless steel autoclave vessel with Teflon-lining for a period of 24 h at a temperature of 200 °C. The resulting precipitate was filtered, washed with ethanol and deionized water to collect the MoS_2 final product, which is dried at 100 °C for 6 h. Electrodes fabrication was done via mixing the active material, polyvinylidene fluoride (PVDF) binder, using a 9:1 mass ratio with an N-methylpyrrolidone (NMP) solution to obtain a slurry which was coated on pre-cleaned nickel foam templates. The as-prepared electrodes were subjected to drying at 70^0 C to ensure completely evaporation of the NMP for 8 hours. The electrochemical analysis of the asymmetric device (ACC//MoS_2) was performed in a two electrode cell fixture, using a microfiber glass filter paper separator submerged in a gel electrolyte (Farshad Barzegar et al. 2015; Barzegar et al. 2016). All electrochemical studies were performed on a Bio-logic VMP-300 potentiostat test system.

3. Results and discussion

Unique morphology of the ACC and MoS2 samples were observed by scanning electron microscopy (SEM) method as displayed in Figure 1. The SEM image of the ACC materials presented in Figure 1 (a) shows the pores present which provides a large ion-accessible surface useful for fast ion transport resulting in high-performance devices. Figure 1 (b) depicts the MoS2 containing coagulated interleaving nano-platelets with thicknesses ranging between 10 - 30 nm.

Figure 2 (a) displays the N_2 adsorption-desorption isotherms of ACC and MoS_2. The ACC material exhibits a type II isotherm based on the IUPAC isotherm classification with an

H4 hysteresis loop while a type III isotherm is observed for the MoS_2 material, signifying a complex structure containing a mixture of both micropores and mesopores. Figure 2 (b) displays the XRD profile for ACC and MoS_2 powder. A Co-Kα, 1.·7890 Å wavelength was used for the XRD analysis. For the ACC sample, a peak at 52° is observed and is assigned to the 101 plane of graphite. The wide peak is a hint that the structure of the material is amorphous. The MoS_2 pattern shows a peak at 10° corresponding to a strong (001) diffraction peak of MoS_2 sample.

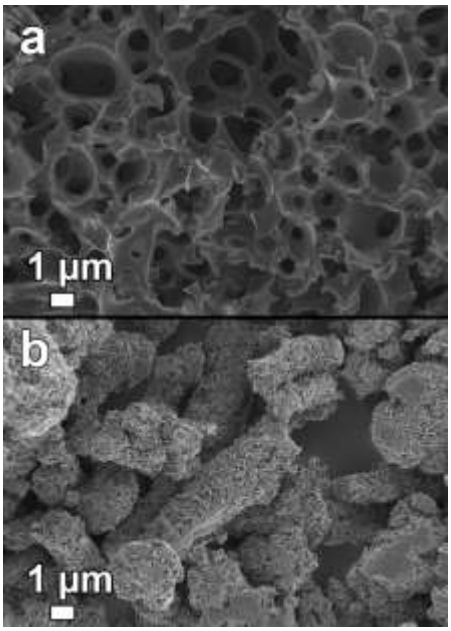

Figure 1. SEM image of (a) ACC and (b) MoS_2

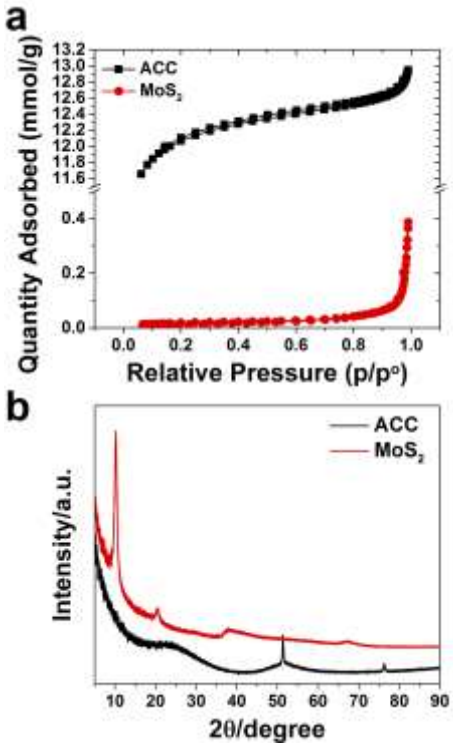

Figure 2. (a) N2 adsorption-desorption isotherm and (b) X-ray diffraction pattern of ACC and MoS_2

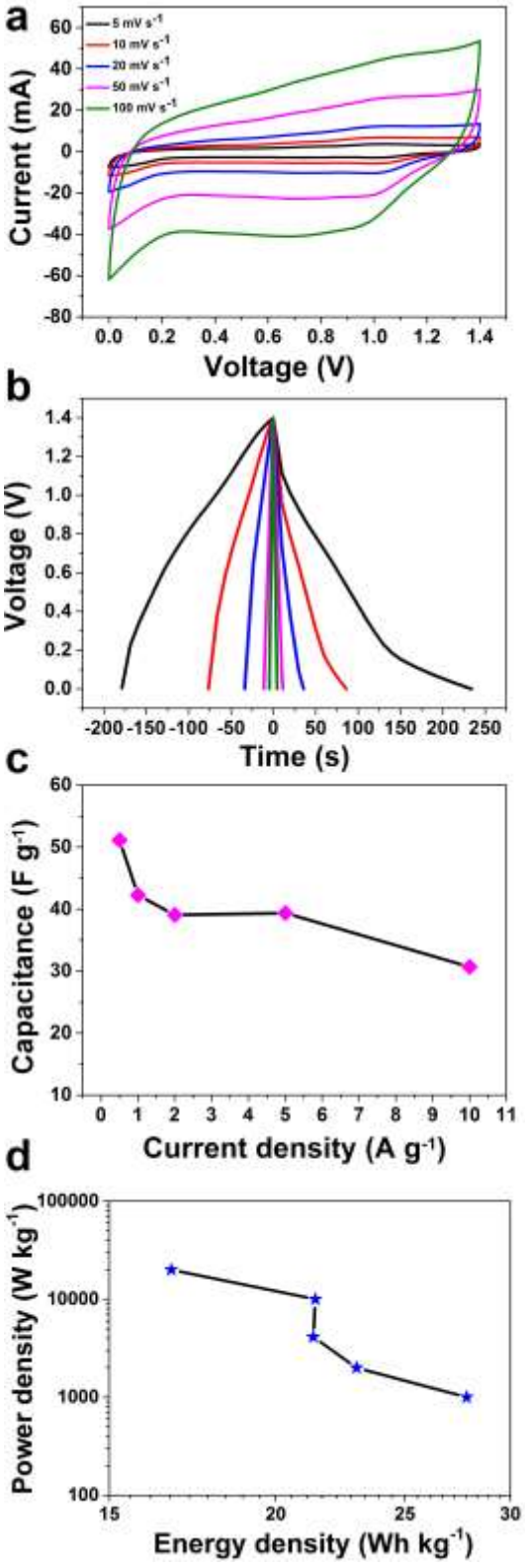

Figure 3. (a) CV plots of the cell at 5 - 100 mV s^{-1} scan rates, (b) GCD curves at gravimetric current density values of 0.5 - 10 A g^{-1}, (c) plot showing the specific capacitance in relation to the current density and (d) Ragone plot for ACC/MoS_2 cell

Figure 3 (a) displays the CV curves for the (ACC/MoS_2) asymmetric cell obtained at varying scanning rates of 5-100 mV s^{-1}. A distorted rectangular shape is observed indicating a

typical pseudocapacitive behavior. This shape is due to the intercalation of K^+ into the MoS_2 electrode during the charging process and the de-intercalation during the reverse process.

Galvanostatic charge/discharge (GCD) plots for the ACC/MoS_2 device at increasing specific current from 0.5-10 A g^{-1} are illustrated in Figure 3 (b). These currents were normalized by the mass of both ACC and MoS_2 in the hybrid device. The specific discharge capacitance and energy, calculated by integrated the area under the GD curve using the following equations (Laheäär et al. 2015), $E_s = I \int Vdt / m3.6$ and $C_s = 2I \int Vdt / m\Delta V^2$. Specific capacitance value of 51 F g^{-1} was calculated at a 0.5 A g^{-1} specific gravimetric current and this decreased to a capacitance of 30.5 F g^{-1} at a high current density of 10 A g^{-1} as shown in Figure 3 (c). The Ragone plot for the asymmetric cell is shown in Figure 3 (d). The maximum energy density of the device was calculated as 27.82 Wh kg^{-1} and related power density of 1000 W Kg^{-1} at a 0.5 A g^{-1} current density. These results are reasonable and are amongst the highest reported for activated carbon based on coconut shell and MoS_2.

One of the main parameters for valuation of a supercapacitor device is long cycle life. Hence, the asymmetric cell was subjected to a continuous current charge-discharge for about 10,000 cycles at a current density of 2 A g^{-1} to test the cycle lifetime of the hybrid cell. The device showed no coulombic efficiency loss after 10,000 cycles at a 2 A g^{-1} gravimetric current density as shown in Figure 4 (a). The excellent coulombic efficiency could be possibly due to the repeated intercalation/de-intercalation into the inner spaces between the cavities of the electrode material and therefore, produces extra available surface area for ions access to electrodes necessary to take full advantages of the surface area by intercalation (Cheng et al. 2011). The CV curves of the device at a 10 mV s^{-1} scan rate before and after cycling test are displayed in Figure 4 (b). The quite resistive CV curves obtained after the 10,000th cycle implying there was a structural change to the morphological electrode material structure due to the continuous cycling.

Electrochemical impedance spectroscopy (EIS) analysis were completed in a 100 kHz - 10 MHz frequency range and the observations from the tests before and after cycling are shown in Figure 4 (c). The Nyquist plot presents a typical capacitive shape with a partial semi-circle in a region of high frequency and almost vertical line in the region of low-frequency. At high frequency, the intercept on the real axis (Z') gives information about the Ohmic resistance (R_s) also known as equivalent series resistance (ESR) of the device. The ESR resistance value combines the intrinsic electrolyte resistances, hybrid material electrodes, and the electrode contact with the outside circuit (Luo et al. 2013). From the Nyquist plot above the device has R_s-value of 1.0 Ω. This small R_s-value proves that the current can easily diffuse through the electrode-electrolyte interface due to the high mobility of K+ cation. However, because of further increases in diffusion path length after cycling test, the R_s value also increases to 2.0 Ω. The repeated effect of cycling such as voltage drop increase, polarization, and insufficient active material/less utilization during cycling affected the results after cycling. Finally, Figure 4 (d) displays the plot of phase angle versus frequency. The first point of the phase angle is ~-76°, which is close to -90° that describes an ideal capacitive response.

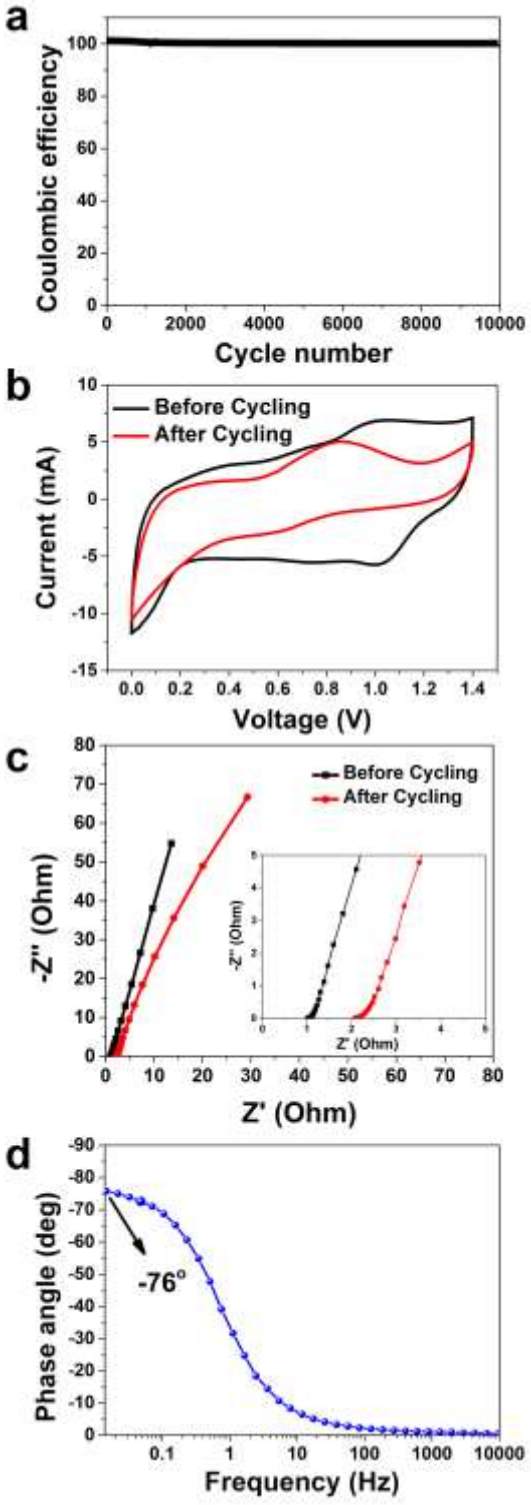

Figure 4. (a) Cycle stability of the cell at a 2 A g^{-1} gravimetric current density (b) CV profile at 10 mV s^{-1} scan rate before and after cycling, (c) EIS plot before and after cycling and (d) the phase angle versus frequency of ACC/MoS_2 device

4. CONCLUSIONS

These results recommend that the ACC/MoS_2 asymmetric cell has high potential to be as a SCs cell in hybrid energy storage system for EVs application. A specific energy of ~ 27.82 Wh Kg^{-1} was reported for the hybrid asymmetric cell at a 0.5 A g^{-1} gravimetric current density with a related specific power of 1000 W kg^{-1} and very good cycle stability. High power and good cycle stability that necessary for EVs are present in ACC/MoS_2 cell and can be investigated in the real device in future.

6. ACKNOWLEDGMENT

This research is co-sponsored by the National Research Foundation of South Africa (Grant Number: 61056). All findings, conclusion or recommendation expressed in this work are solely that of the author(s). The NRF does not accept liability in any regard.

REFERENCES

Barzegar, F. et al., 2015. Asymmetric supercapacitor based on an α-MoO 3 cathode and porous activated carbon anode materials. *RSC Adv.*, 5(47), pp.37462–37468.

Barzegar, F. et al., 2016. Cycling and floating performance of symmetric supercapacitor derived from coconut shell biomass. *AIP Advances*, 6(11).

Barzegar, F. et al., 2015. Effect of conductive additives to gel electrolytes on activated carbon-based supercapacitors. *AIP Advances*, 5(9), p.97171.

Bello, A. et al., 2015. Electrochemical Studies of Microwave Synthesised Bimetallic Sulfides Nanostructures As Faradaic Electrodes. *Electrochimica Acta*, 174, pp.778–786.

Chen, L. et al., 2010. Synthesis and pseudocapacitive studies of composite films of polyaniline and manganese oxide nanoparticles. *Journal of Power Sources*, 195(11), pp.3742–3747.

Cheng, Q. et al., 2011. Graphene and nanostructured MnO2 composite electrodes for supercapacitors. *Carbon*, 49(9), pp.2917–2925.

Conway, B.E., 1999. *Electrochemical Supercapacitors: Scientific Fundamentals and Technological Applications*, New York: Kluwer Academic/Plenum.

Frackowiak, E., 2007. Carbon materials for supercapacitor application. *Physical chemistry chemical physics : PCCP*, 9(15), pp.1774–85.

Jose, R. et al., 2016. Supercapacitor Electrodes Delivering High Energy and Power Densities. *Materials Today: Proceedings*, 3, pp.S48–S56.

Laheäär, A. et al., 2015. *Appropriate methods for evaluating the efficiency and capacitive behavior of different types of supercapacitors*,

Li, R. et al., 2015. Ni3S2@CoS core-shell nano-triangular pyramid arrays on Ni foam for high-performance supercapacitors. *Physical chemistry chemical physics : PCCP*, 17(25), pp.16434–42.

Li, R. et al., 2016. NiCo2S4@Co(OH)2 core-shell nanotube arrays in situ grown on Ni foam for high performances asymmetric supercapcitors. *Journal of Power Sources*, 312, pp.156–164.

Luo, J., Jang, H.D. & Huang, J., 2013. Effect of sheet morphology on the scalability of graphene-based ultracapacitors. *ACS nano*, 7(2), pp.1464–71.

Patil, U.M. et al., 2015. Nanostructured pseudocapacitive materials decorated 3D graphene foam electrodes for next generation supercapacitors. *Nanoscale*, 7, pp.6999–7021.

Ray, R.S. et al., 2015. Fabrication and characterization of titania nanotube/cobalt sulfide supercapacitor electrode in various electrolytes. *Chemical Engineering Journal*, 260, pp.671–683.

Sato, Y. et al., 2000. Electrochemical Behavior of Activated-Carbon Capacitor Materials Loaded with Ruthenium Oxide. *Electrochemical and Solid-State Letters*, 3(3), pp.113–116.

Simon, P. & Gogotsi, Y., 2008. Materials for electrochemical capacitors. *Nature materials*, 7(11), pp.845–854.

Soon, J.M. & Loh, K.P., 2007. Electrochemical Double-Layer Capacitance of MoS[sub 2] Nanowall Films. *Electrochemical and Solid-State Letters*, 10(11), p.A250.

Wang, W. et al., 2014. Hydrous ruthenium oxide nanoparticles anchored to graphene and carbon nanotube hybrid foam for supercapacitors. *Scientific reports*, 4(ii), p.4452.

Zhang, H. et al., 2008. Growth of manganese oxide nanoflowers on vertically-aligned carbon nanotube arrays for high-rate electrochemical capacitive energy storage. *Nano letters*, 8(9), pp.2664–8.

Zheng, J.P., 1999. Ruthenium Oxide-Carbon Composite Electrodes for Electrochemical Capacitors. *Electrochemical and Solid-State Letters*, 2(8), p.359.